Available online at www.sciencedirect.com

SciVerse ScienceDirect

Ceramics International 39 (2013) 7773–7778

CERAMICS INTERNATIONAL

www.elsevier.com/locate/ceramint

MnO nanoparticles with textured porosity supported on mesoporous carbons

Peng Li[a], Yan Song[b,*], Zhihong Tang[a], Guangzhi Yang[a], Quangui Guo[b],
Lang Liu[b], Junhe Yang[a,*]

[a]University of Shanghai for Science and Technology, School of Materials Science and Engineering, Shanghai 200093, China
[b]Key Laboratory of Carbon Materials, Institute of Coal Chemistry, Taiyuan 030001, China

Received 22 January 2013; received in revised form 16 February 2013; accepted 12 March 2013
Available online 21 March 2013

Abstract

Ordered mesoporous carbons doped with MnO nanoparticles (DCs) have been prepared by direct carbonization of a composite of a reverse copolymer-low-molecular-weight phenolic resin dipped in aqueous $Mn(NO_3)_2$ solution. The microstructure of the DCs was analyzed by the small-angle X-ray scattering, X-ray diffraction, nitrogen adsorption isotherms and transmission electron microscopy. The results showed that the size of MnO nanoparticles dispersed on the surface of DCs was about 10–50 nm and the pore size of DCs could be tailored from 4.9 to 9.3 nm as the amount of phenolic resin varied. Moreover, the structure of the DCs obtained was stripe-like at low amount of phenolic resin. However, the structure of the DCs becomes disordered as the amount of phenolic resin increases. Because of its nontoxic nature and cost-effective synthesis, these DCs exhibit properties that are needed for an environment-friendly catalyst and electrode materials.

Keywords: Hybrid mesoporous carbons; Soft-template; Pore size and structure control

1. Introduction

Mesoporous carbon materials have many unique properties such as high surface area, high chemical stability and high conductivity [1–3] that make them have potential application in many potential fields including macromolecules or heavy metal ion adsorption/separation [4–6], catalyst support [7,8], energy storage and conversion [9,10] and so on. Conventionally, mesoporous carbon materials were prepared by the hard templating method and have obtained great success in pore size and structure control [11–16]. For example, the hierarchical porous graphitic carbon materials were prepared using $Ni(OH)_2$ as hard template and phenolic resin as carbon precursor by Cheng et al. [11]. Babić synthesized new mesoporous carbon through curing the SBA-15/carbon cryogel nanocomposites by the hard templating procedure [15,16]. However, because of the disadvantages such as cost, long time and environment polluted. Therefore, scientists were always trying to find an alternative method to synthesize the mesoporous carbons with controllable pore size and structure [17–19]. Fortunately, inspired from the synthesis of mesoporous silica by the soft-templating strategy, this strategy has also been employed to synthesize mesoporous carbons and has also made numerous achievements [20–34]. Up to now, various mesoporous carbon materials including p6mm [20,22], $Im\overline{3}m$ [21], $Ia\overline{3}d$ [23], $Fm\overline{3}m$ [24] and $Fd\overline{3}m$ [33] symmetries have been synthesized by the soft-template strategy with triblock copolymers as structure directing agent.

Recently, hybrid supercapacitors have received considerable attention owing to their high specific power and longer life cycle compared to rechargeable batteries and higher specific energy compared to conventional capacitors [35–42]. Among them, mesoporous carbons doped with MnO_x based supercapacitors can store energy through either or both of double capacitance (adsorption/desorption of ions at the electrode/electrolyte interface) and pseudocapacitance (intercalation/deintercalation of cations into/from the oxide lattices) accompanied by the redox reactions [40–42]. Furthermore, MnO_x are popular because of their abundant resources, affordable production and low environmental impact and have been used

---

*Corresponding authors. Tel./fax: +86 021 55271689.
E-mail addresses: yansong1026@126.com (Y. Song), jhyang@usst.edu.cn (J. Yang).

0272-8842/$ - see front matter © 2013 Elsevier Ltd and Techna Group S.r.l. All rights reserved.
http://dx.doi.org/10.1016/j.ceramint.2013.03.036

in other applications such as electrode materials of lithium battery [43], catalysts [44], capacitive deionization [45] and sensors [46]. However, very few papers have done the work on mesoporous carbons doped with MnO nanoparticles (DCs), which may lead to some interesting application area such as supercapacitors and lithium-ion battery under consideration of combination by the advantages of mesoporous carbons and MnO nanoparticles [47]. Therefore, it still remains a great challenge to prepare DCs with high quality mono-phase MnO nanoparticles due to the uncontrollable phase transformation of multivalent manganese oxides.

In this study, we present a facile method to synthesize the DCs by direct carbonization of a composite of a reverse copolymer-low-molecular-weight phenolic resin dipped in aqueous $Mn(NO_3)_2$ solution. Furthermore, the amount of phenolic resin on the pore size and structure of DCs was studied. This protocol is easy, repeatable.

2. Experimental

2.1. Synthesis of DCs

General procedure: typically (DCs-1), 1.0 g of copolymer ($PO_{97}EO_{186}PO_{97}$) was dissolved in 15 g ethanol under magnetic stirring at 30 °C. Low-molecular-weight phenolic resol precurors were prepared as previously reported with some modification [21,33]. A typical procedure is as follows: 0.5 g of phenol was melted at 45 °C before 0.1 g of NaOH aqueous (20 wt%) was added into it with stirring. 1.1 g of formalin (37–40 wt%) was added dropwise, and the mixture was stirred at 75 °C for 60 min. After cooling the mixture to room temperature, the pH of the reaction was adjusted to neutral (7.0) using 2.0 M HCl aqueous solution. Water was then removed under vacuum below 50 °C for 2 h. and was added dropwise to the above ethanol solution containing copolymer, further stirred for 10 min. The solution was transferred to a dish and the ethanol evaporated at room temperature over 8 h to produce a transparent membrane. The membrane was cured at 100 °C for 24 h in air for further thermopolymerization. Then the membrane was dipped into the aqueous $Mn(NO_3)_2$ solution for 8 h and taken out and it was cured at 100 °C for 10 h. Finally, the product was carbonized at 800 °C for 2 h, with a heating rate of 1 °C min^{-1} under nitrogen atmosphere. (These samples were abbreviated as DCs-*X*, *X*=1, 2, 3 and 4, they were nominated corresponding to the different weight compositions were in the range of phenol/formaldehyde/NaOH/template=0.5:0.42:0.04:1, 0.8:0.77:0.07:1, 1.2:1.0:0.10:1, 1.5:1.26:0.13:1).

2.2. Characterization of DCs

Small angle X-ray scattering (SAXS) recorded by using an imaging plate with X-ray wavelength of λ=1.38 Å at beam line 4B9A of the Beijing Synchrotron Radiation Facility. The X-ray powder diffraction (XRD) patterns of the products were provided using a Bruker D8 advanced X-ray diffractometer equipped with graphite-monochromatized Cu Kα radiation (λ=1.5418 Å). Transmission electron microscopy (TEM) measurement was conducted by using a Hitachi H-800. The samples were prepared by dispersing the products in ethanol with an ultrasonic bath for 30 min and then a few drops of the resulting suspension were placed on a copper grid. Nitrogen adsorption–desorption isotherms were performed at 77 K on a TriStar 3000 volumetric adsorption system. The specific surface area was calculated from the adsorption data in the relative pressure interval from 0.05 to 0.35 using the Brunauer–Emmett–Teller (BET) method. The pore size distribution curve was obtained from adsorption branch by using the Barrett–Joyner–Halenda (BJH) method. The total pore volume (V_{total}) was calculated at the relative pressure of 0.99. The micropore volume (V_{micro}) was determined by t-plot model, and the mosoporous volume (V_{meso}) was calculated by the difference of V_{total} and V_{micro}.

3. Results and discussion

Fig. 1 shows the SAXS patterns of samples prepared under addition of various amounts of phenolic resin. It can be seen that the microstructure of DCs varies as the different amounts of phenolic resin are used. For example, for DCs-1–2 with the ratio 0.5:0.42:0.04:1 or 0.8:0.77:0.07:1, both samples give one sharp peak in the small angle area suggesting these two samples have ordered structure. However, when the ratio increases to 1.2:1.0:0.10:1 or 1.5:1.26:0.13:1 for DCs-3–4, both of them show wide peaks in small angle area suggesting the pore structure of them becomes disordered.

We use XRD measurements as a qualitative analytical tool for phase identification of MnO nanoparticles of the DCs-*X* shown in Fig. 2. Five characteristic peaks with marked crystal faces at 2θ=34.9°, 40.6°, 58.6°, 70.2° and 73.7° can be assigned to be (111), (200), (220), (311) and (222) planes, which are in good agreement with the cubic Fm3m (225) space group MnO (JCPDSC no. 07-0230), cell parameters: a=0.4445 nm. The (200) peak is very strong, which may be due to the perfect crystalline of MnO nanoparticles. No

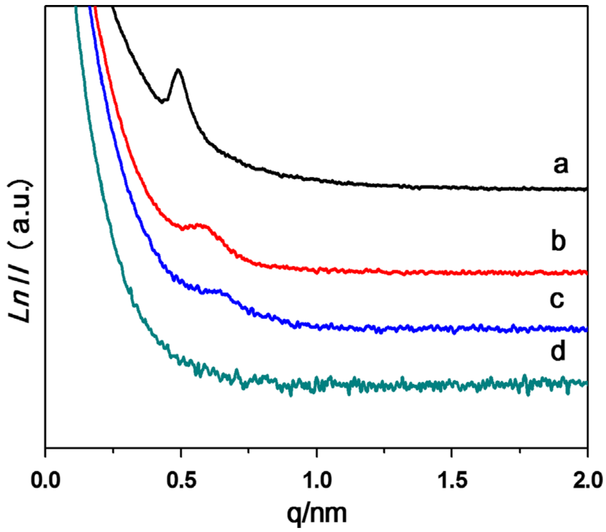

Fig. 1. SAXS patterns of DCs-*X* prepared under various amounts of phenolic resin.

reflection related to $Mn(NO_3)_2$ and carbon was observed, indicating that dispersing the MnO nanoparticles on the surface of mesoporous carbons was achieved and the amorphism of the pore wall of the DCs which is also the phenomenon for most mesoporous materials.

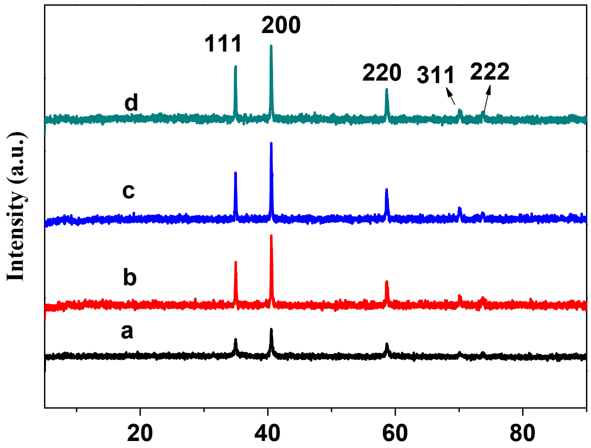

Fig. 2. XRD patterns of DCs-*X* prepared under various amounts of phenolic resin.

Fig. 3 shows the typical TEM images of DCs-1. Stripe-like pore structure can be observed from this sample shown in Fig. 3a and b, indicating that the DCs-1 has ordered pore structure. The grain size of MnO nanoparticles is about 10–50 nm but they are not evenly distributed on the pore wall of mesoporous carbons. The high-resolution TEM image (shown in Fig. 3c) and corresponding Fourier diffractograms fourier transform the selected area (shown in Fig. 3d) show the detailed structure of the MnO nanoparticles. The spacing of the clear lattice fringes in Fig. 3c was found to be about 0.256 nm, which was coincident with the (111) d-value of MnO. The TEM images of DCs-2 are demonstrated in Fig. 4. It can be seen that DCs-2 also has the ordered stripe-like pore structure. The grains particles are about 50 nm even while dispersed on the surface of mesoporous carbons. Fig. 4c and d shows the detailed structure of MnO nanoparticles, and the lattice fringes that can be clearly distinguished confirming the crystalline nature of MnO nanoparticles as well.

The formation mechanism of MnO nanoparticles can be understood by considering the chemical reaction during the carbonization process. $Mn(NO_3)_2$ was decomposed at high temperature, according to the following reaction: 2Mn\(NO3) $_2 \rightarrow 2MnO + 2NO_2 + O_2$. Meanwhile, the oxygen

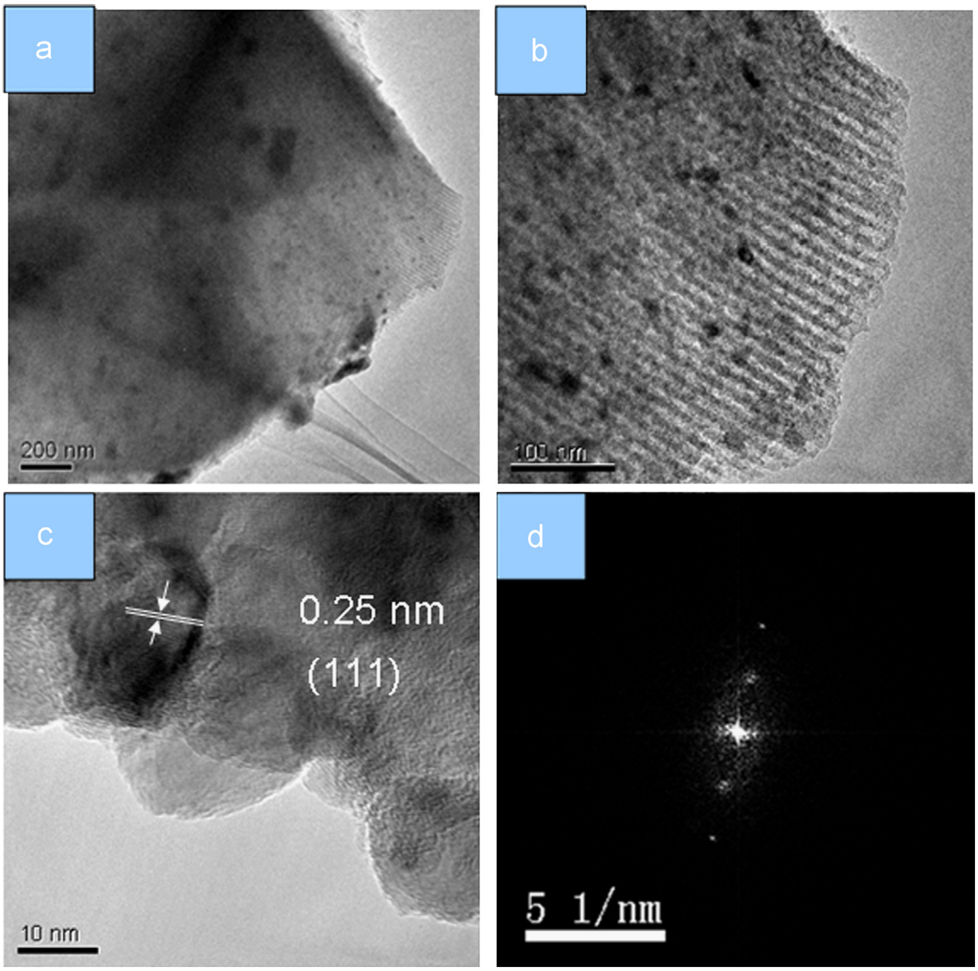

Fig. 3. TEM images of DCs-1.

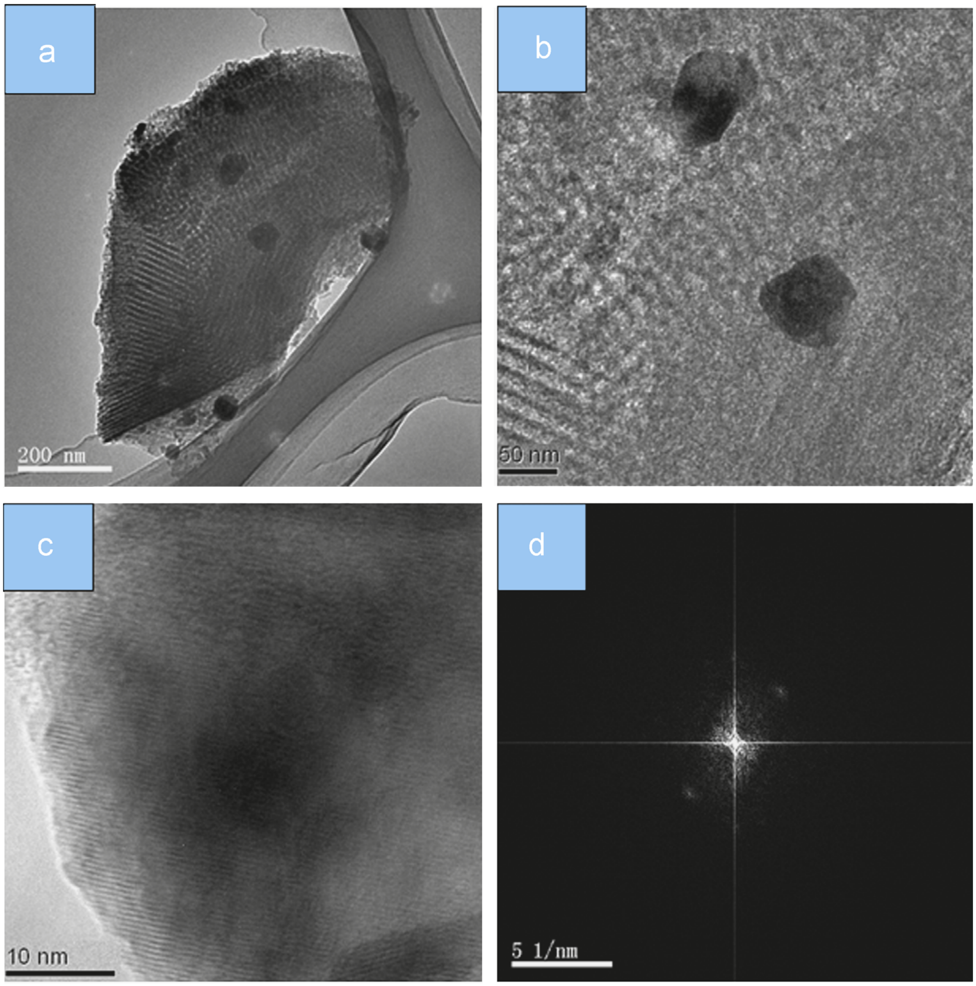

Fig. 4. TEM images of DCs-2.

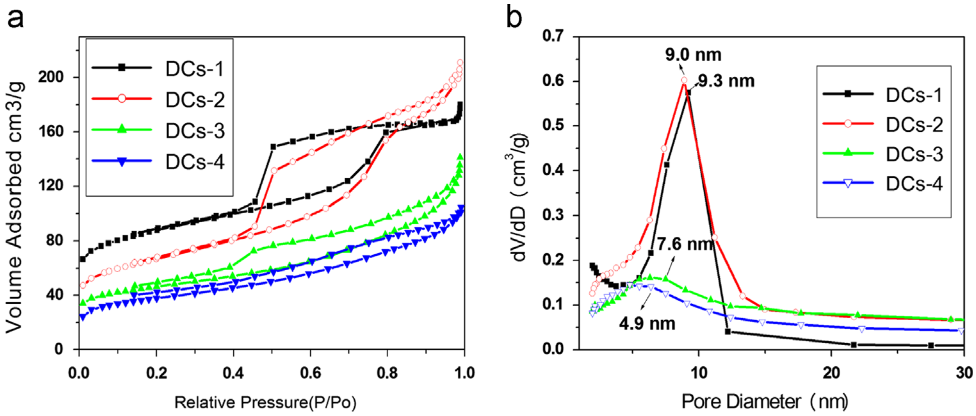

Fig. 5. N_2 adsorption/desorption isotherms (a) and the corresponding BJH pore size distribution and (b) of DCs-*X* prepared under various amounts of phenolic resin.

may react with the mesoporous carbons. That is to say the oxygen possibly also has the effect of expanding the pore size of mesoporous carbons during the carbonization.

Fig. 5(a) shows the nitrogen adsorption/desorption isotherms of the DCs-*X*. All samples have the typical IV type hysteresis, indicating that the samples are characteristic mesoporous materials. The corresponding BJH pore size distributions are shown in Fig. 5(b). It can be observed that the pore size distribution can be tailored from 4.9 to 9.3 nm as the amount of phenolic resin increases, which is different from that of ordered mesoporous carbons previously reported [33], further confirming the effects of expanding the pore size of

Table 1
Pore parameters of DCs-*X* prepared under various amounts of phenolic resin.

Sample	S_{BET} (m^2/g)	V_{total} (cm^3/g)	V_{micro} (cm^3/g)	V_{meso} (cm^3/g)	$Ratio_{meso}$ (%)
DCs-1	304	0.28	0.07	0.21	75
DCs-2	234	0.33	0.03	0.30	90
DCs-3	161	0.22	0.03	0.19	86
DCs-4	132	0.16	0.02	0.14	88

$Ratio_{meso} = (V_{total} - V_{micro})/V_{total}$.

mesoporous carbons of oxygen generated by decomposition of $Mn(NO_3)_2$. Table 1 shows the parameters of DCs-*X*, it can be obviously observed that the obtained DCs have high surface area and great pore volume. However, the surface area and pore volume decrease as the amount of phenolic resin increase.

4. Conclusion

In conclusion, the DCs with tunable pore size from 4.9 to 9.3 nm have been successfully prepared by direct carbonization of a composite of a reverse copolymer-low-molecular-weight phenolic resin dipped in aqueous $Mn(NO_3)_2$ solution. The results showed that the structure of the DCs obtained has the transformation from stripe-like structure to disordered structure. The DCs possess great potential applications in catalysis, separation and energy storage and conversion fields.

Acknowledgments

The research was supported by the financial support of the National Nature Science Fund of China (50602046), ICC CAS Fund for distinguished Young Scientist, State Education Ministry and Natural Science Fund of Shanxi Province (2007011075). The authors thank Fund of Testing from Institute of High Energy and Physics for SAXS measurements assistance.

References

[1] C. Liang, Z. Li, S. Dai, Mesoporous carbon materials: synthesis and modification, Angewandte Chemie International Edition 47 (2008) 3696–3717.

[2] Y. Zhai, Y. Dou, D. Zhao, P.F. Fulvio, R.T. Mayes, S. Dai, Carbon materials for chemical capacitive energy storage, Advanced Materials 23 (2011) 4828–4850.

[3] M. Inagaki, H. Konno, O. Tanaike, Carbon materials for electrochemical capacitors, Journal of Power Sources 195 (2010) 7880–7903.

[4] P.S. Tin, H.Y. Lin, R.C. Ong, T.-S. Chung, Carbon molecular sieve membranes for biofuel separation, Carbon 49 (2011) 369–375.

[5] G. Liu, S. Zheng, D. Yin, Z. Xu, J. Fan, F. Jiang, Adsorption of aqueous alkylphenol ethoxylate surfactants by mesoporous carbon CMK-3, Journal of Colloid and Interface Science 302 (2006) 47–53.

[6] K. Yang, B. Xing, Adsorption of organic compounds by carbon nanomaterials in aqueous phase: Polanyi theory and its application, Chemical Record 110 (2010) 5989–6008.

[7] G. Chai, S.B. Yoon, S. Kang, J.H. Choi, Y.E. Sung, Y.S. Ahn, H.S. Kim, J.S. Yu, Ordered uniform porous carbons as a catalyst support in a direct methanol fuel cell, Electrochimica Acta 50 (2004) 823–826.

[8] Z.Z. Jiang, Z.B. Wang, D.M. Gu, E.S. Smotkin, Carbon riveted Pt/C catalyst with high stability prepared by in situ carbonized glucose, Chemical Communications 46 (2010) 6998–7000.

[9] K. Xie, X. Qin, X. Wang, Y. Wang, H. Tao, Q. Wu, L. Yang, Z. Hu, Carbon nanocages as supercapacitor electrode materials, Advanced Materials 24 (2011) 347–352.

[10] N. Brun, S.R.S. Prabaharan, C. Surcin, M. Morcrette, H. Deleuze, M. Birot, O. Babot, M.-F. Achard, R. Backov, Design of hierarchical porous carbonaceous foams from a dual-template approach and their use as electrochemical capacitor and Li ion battery negative electrodes, Journal of Physical Chemistry C 116 (2012) 1408–1421.

[11] D.W. Wang, F. Li, M. Liu, G.Q. Lu, H.M. Cheng, 3D aperiodic hierarchical porous graphitic carbon material for high-rate electrochemical capacitive energy storage, Angewandte Chemie International Edition 47 (2008) 373–376.

[12] S. Reculusa, B. Agricole, A. Derré, M. Couzi, E. Sellier, P. Delhaès, S. Ravaine, Colloidal crystals as templates for macroporous carbon electrodes of controlled thickness, Electroanalysis 19 (2007) 379–384.

[13] C.M. Yang, C. Weidenthaler, B. Spliethoff, M. Mayanna, F. Schuth, Facile template synthesis of ordered mesoporous carbon with polypyrrole as carbon precursor, Chemistry of Materials 17 (2005) 355–358.

[14] L. Zhi, J. Wang, G. Cui, M. Kastler, B. Schmaltz, U. Kolb, U. Jonas, K. Müllen, from well-defined carbon-rich precursors to monodisperse carbon particles with hierarchic structures, Advanced Materials 19 (2007) 1849–1853.

[15] B. Babić, M. Kokunešoski, M. Miljković, B. Matović, J. Gulicovski, M. Stojmenović, D. Bučevac, New mesoporous carbon materials synthesized by a templating procedure, Ceramics International 39 (2013) 4035–4043.

[16] B. Babić, M. Kokunešoski, M. Miljković, M. Prekajski, B. Matović, J. Gulicovski, D. Bučevac, Synthesis and characterization of the SBA-15/carbon cryogel nanocomposites, Ceramics International 38 (2012) 4875–4883.

[17] Z. Li, W. Yan, S. Dai, A novel vesicular carbon synthesized using amphiphilic carbonaceous material and micelle templating approach, Carbon 42 (2004) 767–770.

[18] K.T. Lee, S.M. Oh, Novel synthesis of porous carbons with tunable pore size by surfactant-templated sol-gel process and carbonisation, Chemical Communications (2002) 2722–2723.

[19] J. Yamashita, T. Hirano, M. Shioyab, Development of mesopores during activation of poly(vinylidene fluoride)-based carbon, Carbon 40 (2002) 1541–1548.

[20] C. Liang, K. Hong, G.A. Guiochon, J.W. Mays, S. Dai, Synthesis of a large-scale highly ordered porous carbon film by self-assembly of block copolymers, Angewandte Chemie International Edition 43 (2004) 5785–5789.

[21] Y. Meng, D. Gu, F. Zhang, Y. Shi, H. Yang, Z. Li, C. Yu, B. Tu, D. Zhao, Ordered mesoporous polymers and homologous carbon frameworks: amphiphilic surfactant templating and direct transformation, Angewandte Chemie International Edition 44 (2005) 7053–7059.

[22] S. Tanaka, N. Nishiyama, Y. Egashira, K. Ueyama, Synthesis of ordered mesoporous carbons with channel structure from an organic–organic nanocomposite, Chemical Communications 41 (2005) 2125–2127.

[23] Y. Meng, Dong Gu, Fuqiang Zhang, Y. Shi, L. Cheng, D. Feng, Zhangxiong Wu, Z. Chen, Y. Wan, A. Stein, D. Zhao, A family of highly

ordered mesoporous polymer resin and carbon structures from organic–organic self-assembly, Chemistry of Materials 18 (2006) 4447–4464.

[24] C. Liu, L. Li, H. Song, X. Chen, Facile synthesis of ordered mesoporous carbons from F108/resorcinol–formaldehyde composites obtained in basic media, Chemical Communications 43 (2007) 757–759.

[25] Zhiyong Wang, Fan Li, A. Stein, Direct synthesis of shaped carbon nanoparticles with ordered cubic mesostructure, Nano Letters 7 (2007) 3223–3226.

[26] A.-H. Lu, B. Spliethoff, F. Schuth, Aqueous synthesis of ordered mesoporous carbon via self-assembly catalyzed by amino acid, Chemistry of Materials 20 (2008) 5314–5319.

[27] M. Yoshimune, T. Yamamoto, M. Nakaiwa, K. Haraya, Preparation of highly mesoporous carbon membranes via a sol–gel process using resorcinol and formaldehyde, Carbon 46 (2008) 1031–1036.

[28] K. Kailasam, Y.-S. Jun, P. Katekomol, J.D. Epping, W.H. Hong, A. Thomas, Mesoporous melamine resins by soft templating of block-co-polymer mesophases, Chemistry of Materials 22 (2010) 428–434.

[29] M.N. Lee, A. Mohraz, Bicontinuous macroporous materials from bijel templates, Advanced Materials 22 (2010) 4836–4841.

[30] R.T. Mayes, C. Tsouris, J.O. Kiggans Jr, S.M. Mahurin, D.W. DePaoli, S. Dai, Hierarchical ordered mesoporous carbon from phloroglucinol-glyoxal and its application in capacitive deionization of brackish water, Journal of Materials Chemistry 20 (2010) 8674–8678.

[31] D. Nandan, P. Sreenivasulu, S.K. Saxena, N. Viswanadham, Facile synthesis of a sulfonated carbon–silica-meso composite and mesoporous silica, Chemical Communications 47 (2011) 11537–11539.

[32] C.T. Nguyen, D.-P. Kim, Direct preparation of mesoporous carbon by pyrolysis of poly(acrylonitrile-b-methylmethacrylate) diblock copolymer, Journal of Materials Chemistry 21 (2011) 14226–14230.

[33] P. Li, Y. Song, Q. Lin, J. Shi, L. Liu, L. He, H. Ye, Q. Guo, Preparation of highly-ordered mesoporous carbons by organic-organic self-assembly using the reverse amphiphilic triblock copolymer PPO–PEO–PPO with a long hydrophilic chain, Microporous and Mesoporous Materials 159 (2012) 81–86.

[34] Y. Wang, B. Li, C. Zhang, X. Song, H. Tao, S. Kang, X. Li, A simple solid–liquid grinding/templating route for the synthesis of magnetic iron/graphitic mesoporous carbon composites, Carbon 51 (2013) 397–403.

[35] J. Bae, M.K. Song, Y.J. Park, J.M. Kim, M. Liu, Z.L. Wang, Fiber supercapacitors made of nanowire–fiber hybrid structures for wearable/flexible energy storage, Angewandte Chemie International Edition 50 (2011) 1683–1687.

[36] C. Yuan, L. Yang, L. Hou, J. Li, Y. Sun, X. Zhang, L. Shen, X. Lu, S. Xiong, X.W.D. Lou, Flexible hybrid paper made of monolayer Co_3O_4 microsphere arrays on rGO/CNTs and their application in electrochemical capacitors, Advanced Functional Materials 22 (2012) 2560–2566.

[37] L. Yuan, X.H. Lu, Xu Xiao, T. Zhai, J. Dai, Fengchao Zhang, B. Hu, Xue Wang, Li Gong, Jian Chen, C. Hu, Y. Tong, J. Zhou, Z.L. Wang, Flexible solid-state supercapacitors based on carbon nanoparticles MnO_2 nanorods hybrid structure, ACS Nano 6 (2012) 656–661.

[38] L. Bao, J. Zang, X. Li, Flexible Zn_2SnO_4/MnO_2 core/shell nanocable-carbon microfiber hybrid composites for high-performance supercapacitor electrodes, Nano Letters 11 (2011) 1215–1220.

[39] V.K. Thakur, G. Ding, J. Ma, P.S. Lee, X. Lu, Hybrid materials and polymer electrolytes for electrochromic device applications, Advanced Materials 24 (2012) 4071–4096.

[40] Sheng Chen, Junwu Zhu, Xiaodong Wu, Qiaofeng Han, X. Wang, Graphene oxide MnO_2 nanocomposites for supercapacitors, ACS Nano 4 (2010) 2822–2830.

[41] M.N. Patel, X. Wang, B. Wilson, D.A. Ferrer, S. Dai, K.J. Stevenson, K. P. Johnston, Hybrid MnO_2–disordered mesoporous carbon nanocomposites: synthesis and characterization as electrochemical pseudocapacitor electrodes, Journal of Materials Chemistry 20 (2010) 390.

[42] C. Xu, Y. Zhao, G. Yang, F. Li, H. Li, Mesoporous nanowire array architecture of manganese dioxide for electrochemical capacitor applications, Chemical Communications 45 (2009) 7575–7577.

[43] B. Sun, Z. Chen, H.-S. Kim, H. Ahn, G. Wang, MnO/C core–shell nanorods as high capacity anode materials for lithium-ion batteries, Journal of Power Sources 196 (2011) 3346–3349.

[44] V.B. Boppana, F. Jiao, Nanostructured MnO_2: an efficient and robust water oxidation catalyst, Chemical Communications 47 (2011) 8973–8975.

[45] J. Yang, L. Zou, H. Song, Z. Hao, Development of novel MnO_2/nanoporous carbon composite electrodes in capacitive deionization technology, Desalination 276 (2011) 199–206.

[46] W.S. Seo, H.H. Jo, K. Lee, B. Kim, S.J. Oh, J.T. Park, Size-dependent magnetic properties of colloidal Mn(3)O(4) and MnO nanoparticles, Angewandte Chemie International Edition 43 (2004) 1115–1117.

[47] Y. Tan, C. Xu, G. Chen, X. Fang, N. Zheng, Q. Xie, Facile synthesis of manganese-oxide-containing mesoporous nitrogen-doped carbon for efficient oxygen reduction, Advanced Functional Materials 22 (2012) 4584–4591.